Supplemental Material

Supplemental methods

Conjugation of ACPPs to macromolecules. The peptide was synthesized with $H_2N(CH_2CH_2O)_2CH_2CO$-e_9 instead of Suc-e_8, and was capped with S-trityl-mercaptoacetic acid (Anaspec) while the peptide was still on the synthesis resin. The S-trityl protecting group was removed along with all other protecting groups when the peptide was cleaved off the resin. The crude peptide was purified on HPLC (semi-prep C18 reverse phase column, 15% acetonitrile-30% acetonitrile for 20 min. in water plus 0.05% TFA, 1.8ml/min. flow rate). The purified peptide was labeled with Cy5 mono-NHS ester or DOTA mono-NHS ester through the amino side chain on the C-terminal lysine. The free mercapto group on the N-terminus of the peptide was then reacted with the maleimide group of a heterobifunctional adapter, 2-nitro-4-sulfophenyl maleimidylhexanoate. The 2-nitro-4-sulfophenyl ester (Molecular Biosciences), chosen for its greater solubility and reactivity compared to conventional N-hydroxysuccinimide esters, was finally reacted with an amine group on murine serum albumin, aminodextran, or a 5th-generation PAMAM dendrimer (Dendritech Nanotechnologies Inc). Excess amino groups on the dextran or dendrimer were blocked with succinyl groups or very short PEG chains using succinic anhydride or $MeO(CH_2CH_2O)_3CH_2CH_2CO$-(N-hydroxysuccinimide) respectively. The crude product was purified by Amicon filtration (Millipore, 10 or 30 kDa cutoff) and washed with water 10 times. In general, the mean peptide:macromolecule stoichiometry was approximately 1:1, as determined by weighing the purified product and measuring Cy5 absorbance in the sample.

Computing ratios for epifluorescence images of mice. Region analysis (average pixel intensity) was done using Adobe Photoshop using regions similar to those shown in Supplemental figure 1.

Technetium experiments for validation of SUV technique. Optical SUV values were done as described above and in Supplemental Figure 2. Technetium-99m experiments were done by labeling Suc-e_9-xPLG(MeC)Ax-r_9-k(DTPA) (MeC = methylcysteine) peptide with technetium-99m and injecting the probe intravenously into animals (n=3). Organs were counted using a gamma counter and % ID/g calculated as (counts/weight tissue)/ total counts injected.

Mass Spectrometry. To extract ACPPs to obtain electrospray (ESI) mass spectra, a solution of 9M guanidinium chloride (GuHCL) in 10mM tris-glycine buffer was used to homogenize and dissolve the ACPP from the internal organ tissue of mice. The GuHCl disrupts the binding of ACPP to cell lipids and protein, allowing these components to be removed by thrice extraction with 50:50 chloroform:methanol solution. The sample is then diluted twelve-fold to reduce the [GuHCl] and injected on weak cation exchange (WCX) HPLC. The WCX media was the 12 micron particle PolyCAT A polyaspartamide from PolyLC Inc. It was slurry-packed in a 2mm I.D. by 10cm long PEEK-lined column from Alltech. The fraction containing the peptide is followed by fluorescence emission at 680nm, and the WCX-purified peptide is injected into a ThermoFisher Orbitrap LC-MS with a reverse phase column and an ESI Ionspray mass spectrometer interface.

The ACPP peptide can be detected at a pmol/mg concentration in the original tissue sample, with a detection limit of approximately 1 ppm. Any proteolytic enzymes released from the tissue were presumed to be inactivated by the GuHCl. This was tested by dissolving a previously characterized piece of tissue and spiking it with intact peptide that was then recovered in its full length, uncleaved form in the LC-MS. Good recovery

of the ACPP was found for the WCX column, which bound both cleaved and intact ACPP completely, even in the presence of 0.7 M GuHCl. Diluting the ACPP extract before injection on WCX prevented column blockage from residual tissue lipids.

Zymogram gels. Frozen tissues from tumors were homogenized in PBS at 200 mg/mL. The supernatant was then diluted out 1:10 with 50% tris-glycine SDS sample buffer (Novex, Invitrogen) and run on a pre-cast 10% zymogram gel (Novex, Invitrogen) and processed according to manufacture instructions. After gels were developed they were incubated in 2% Coomassie brilliant blue (MP Biomedicals Inc.) with 40% methanol and 10% acetic acid. Gels were destained in 40% methanol and 10% acetic acid and then imaged on UVP gel imager. HT1080 tissue, PyMT MMP-2 $^{-/-}$, and MMP-9 $^{-/-}$ tissues were used as standards for both human and mouse MMP-2 and -9.

Fluorescence histology of necrosis. Tumors were excised from animals, frozen and sectioned to 20μm. Fluorescence histology imaging was done as described in methods.

Immunohistochemistry of MMPs in mouse tissue.

PyMT frozen tissue sections (10μm) were immunostained using anti-MMP-2 mouse mAB (IM33L, EMD) and anti-MMP-9 mouse mAb (IM61, EMD) at 1:50 dilutions. Primary Ab was treated and Dako kit horseradish peroxidase DAB staining protocol was used for processing sections (Dako).

Supplemental Figure Legends

Supplemental Figure 1. Common strategies in image processing can be deceptive.

(A) Shows raw data from an injected mouse. (B) Shows the same image threshold,

pseudo colored and overlaid back on to the original image. (C) Shows "tumor to background" measurements for three "background" regions indicated in (A), along with the ratio of tumor: background.

Supplemental Figure 2. Tissue specific calibrations for standardized uptake values. (A) Images showing tumor and liver prior to analysis by SUV using standard optical imaging. The tumor appears to be nearly 50% brighter. (B) shows raw SUV calibration data taken at 1s, 700nm with the Maestro mouse imager at level 1. Images were also taken at 300ms and at 3s to be sure that all intensity values were in range for each final concentration tested. All imaging is done on frozen tissue, and images are scaled 0/15 in Photoshop prior to processing. Processing 12 SUV's takes roughly 45 minutes to 1 hour, and involves a single tube with a disposable pestle. These tubes were spiked with different concentrations of r_9-x-k(Cy5) prior to processing and were used to determine calibration factors that relate intensity to amount of Cy5 present. Off peak emission is used because it allows us to excite Cy5 at a longer wavelength (650nm), thereby decreasing absorbance due to hemoglobin and other porphyrins in liver, kidney and spleen. Calibration tubes were also imaged and analyzed for excitation at 620nm. (C) shows the linear relationship between intensity and Cy5 concentration at 700nm; similar curves can be made at 680nm. (D) compares the slopes, or "calibration factors" from four such experiments (mean ± standard deviation), and (E) compares % ID/g (or SUV/weight of animal*100) for a Cy5 labeled peptide and its technetium analogue. Although the correlation is imperfect, especially in the tumor, the SUV assay gives far more predictive results for the radiolabeled peptide than the gross images shown in (A), and provides a means of comparing different types of free peptides.

Supplemental Figure 3. Mass spectrometry of tissue homogenates to confirm cleavage of ACPP substrate *in vivo.* Tumor tissue from mouse injected with (suc-e_8-xPLGLAG-r_9-c(Cy5)), LC-MS retention 16.7min (upper panel). FTMS is shown in lower panel with resolution 30000, displaying centroid peaks.

Supplemental Figure 4. Gelatinases are identified in all tumor types tested by zymogram gel. Tumors from different xenografts that used in this study were homogenized and samples were run on a 10% zymogram gel to assay levels of active MMP-2 and -9. MMP-2 and -9 are identified as well as the position that molecular weight markers ran on the gel. After being developed pictures were taken of the gel.

Supplemental Figure 5. Zymogram gel of PyMT knockout tissues. Gelatinase activity in tumor (A), liver (B) and kidney (C) from PyMT animals and associated knockouts.

Supplemental Figure 6. Uptake of ACPP's into necrotic areas of tumor. (A) Shows a tumor from a B16F10 mouse six hours after injection with the $(PEG\text{-}_2)_2$ probe. (B) shows an H/E image demonstrating that the region taking up the $(PEG_2)_2$ peptide consists of necrotic tissue. This was observed in several tumor types (including MMTV-PyMT). In this case, probe is typically uncleaved on a peptide gel.

Supplemental Figure 7. Antibody staining confirms the localization of gelatinases to tumor stroma and that mostly MMP-2 is present in PyMT tumors.

Supplemental Figure 8: Disappearance of the cartilage uptake with a negative control. (A) shows a mouse injected with the $(PEG_2)_2$ control probe. (B) shows a mouse

injected with a similar probe with alternating arginines and glutamate residues. Note the disappearance of cartilage uptake with the second control probe.

Supplemental Figure 9. Fate of cleavable and control ACPP's in liver, kidney and tumors of wildtype PyMT animals as shown by gel electrophoresis. Tissues were processed and run on 10-20% tricine gels as in Fig. 1D to determine the extent of cleavage of peptides deposited within the tissue. Often there was an arc in the peptide band when the gel was overloaded (tissue homogenate composed of DNA, protein, and lipids). Because different peptides leave very different amounts of fluorescence in the tissue, the gain and offset of each panel have been independently adjusted for maximum contrast, and image gamma has been set to 1.5. These images were generated from PyMT tumor mice in the FVB background, whereas Fig. 1D is from HT1080 tumors in nude mice. We found that the D-amino acid xplglag linker is less cleaved in PyMT tumors than in HT1080 xenografts and that the $(PEG2)_2$ often has regions of higher peptide uptake (possibly due to necrosis). In the tumor panel, each of the duplicate lanes represents a separate mouse.

Supplemental Figure 10. Intratumoral distribution of ACPPs attached to large molecular weight carriers. (A) H/E staining and (B) Cy5 fluorescence from adjacent frozen sections of a PyMT tumor 48 hours after IV injection with cleavable ACPP (e_9-XPLGLAX-r_9-k(Cy5) attached to a PAMAM dendrimer whose excess amino groups were capped by succinyl groups. Note that the dendrimeric ACPP deposits fluorescence as deeply into the tumor and in a similar stromal pattern as do unadorned ACPPs (Fig. 3). (C) Immunostaining for F480, a macrophage marker (FITC-conjugated antibody, 1:50 dilution, Caltag Laboratories). (D) Corresponding Cy5 fluorescence showing considerable colocalization of ACPPs with macrophages. (E) F480 immunostaining and (F) corresponding Cy5 fluorescence of a brightly stained lymph node.

Supplemental Figures

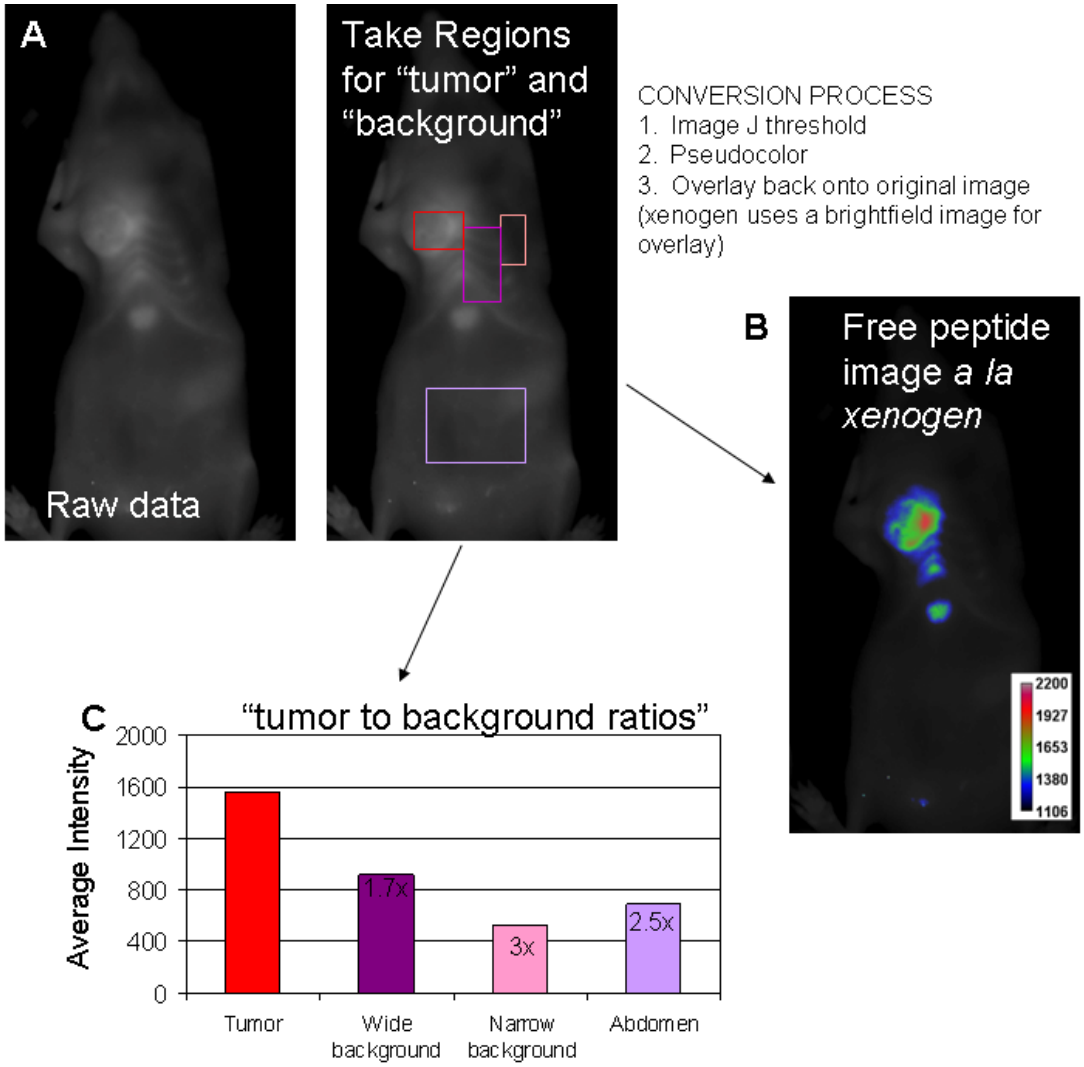

Supplemental Figure 1

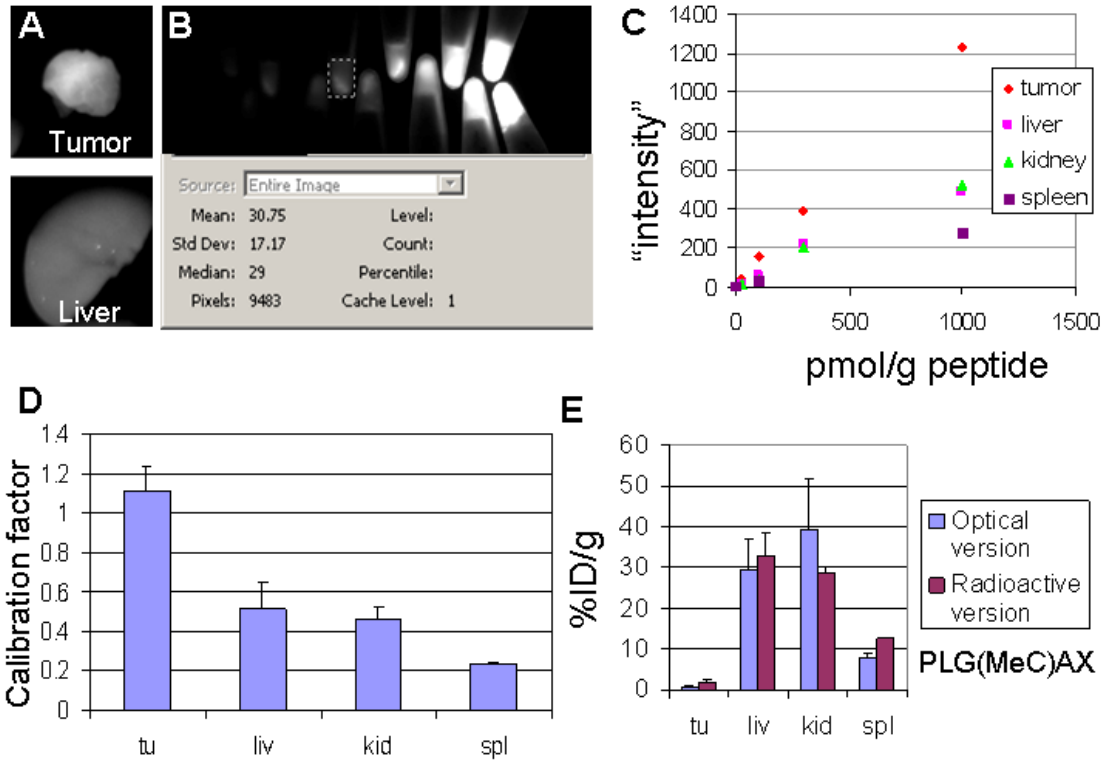

Supplemental Figure 2

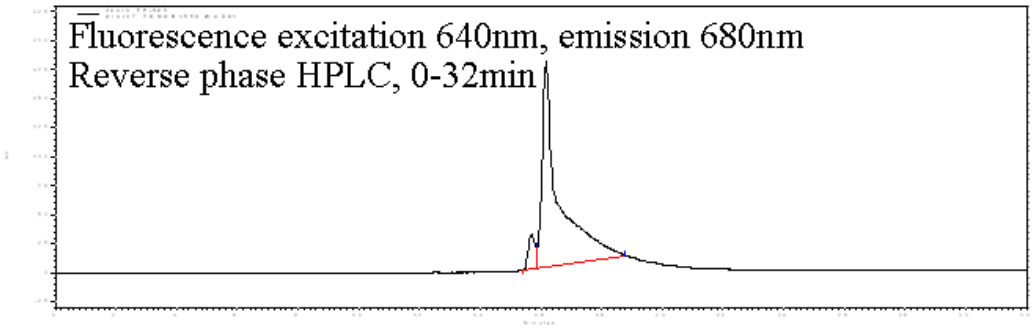

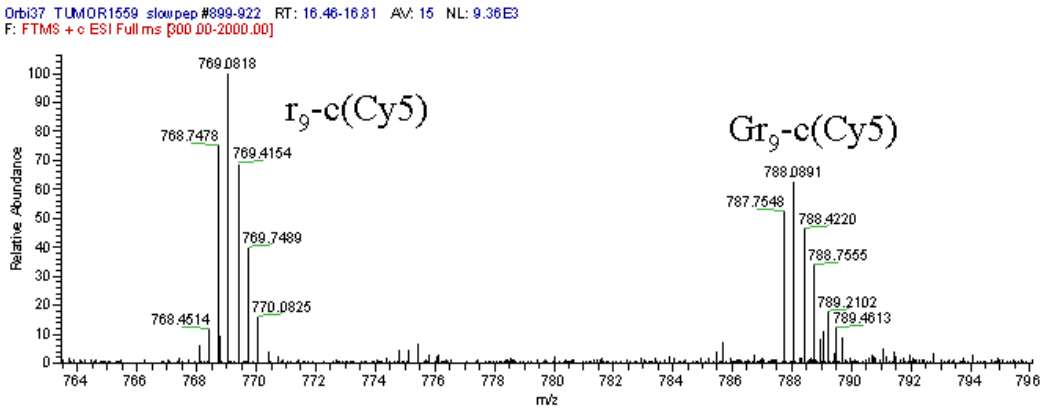

Supplemental Figure 3

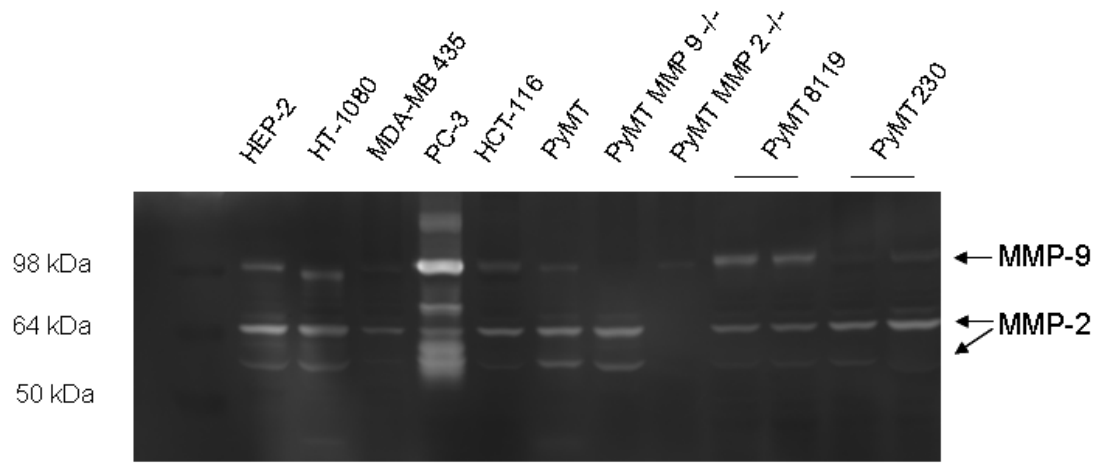

Supplemental Figure 4

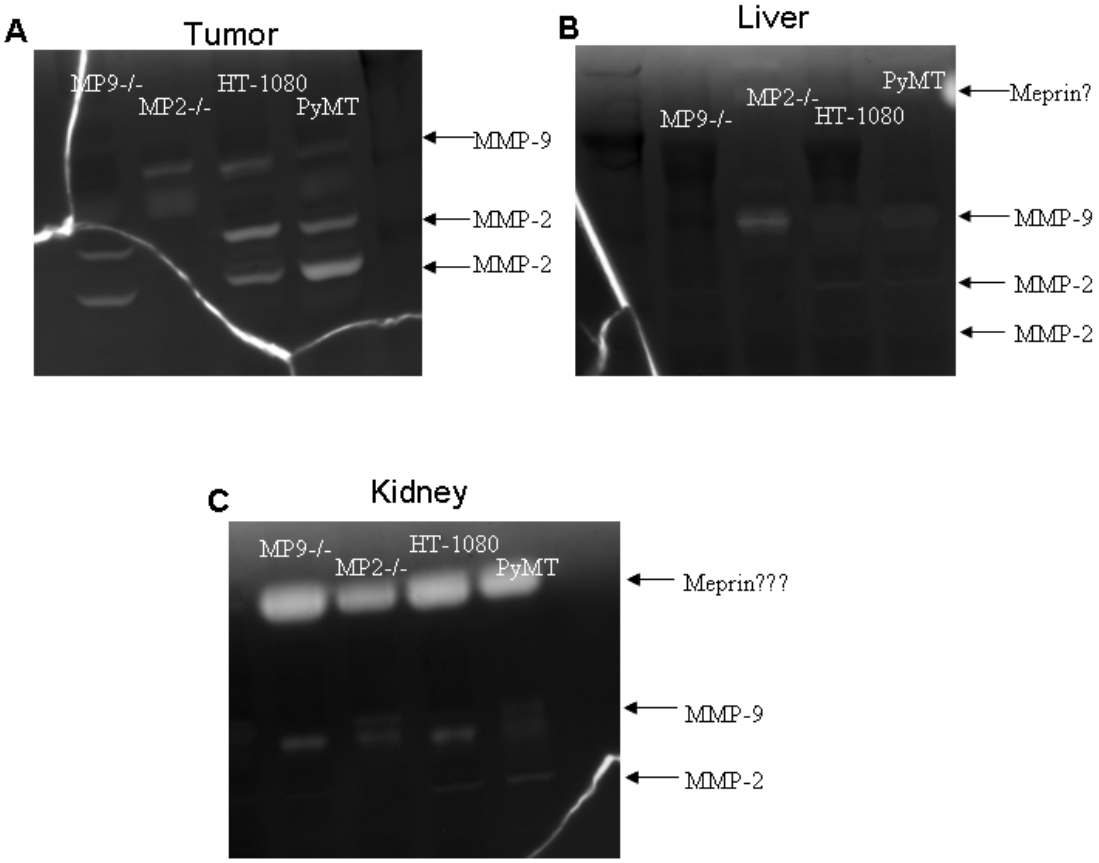

Supplemental Figure 5

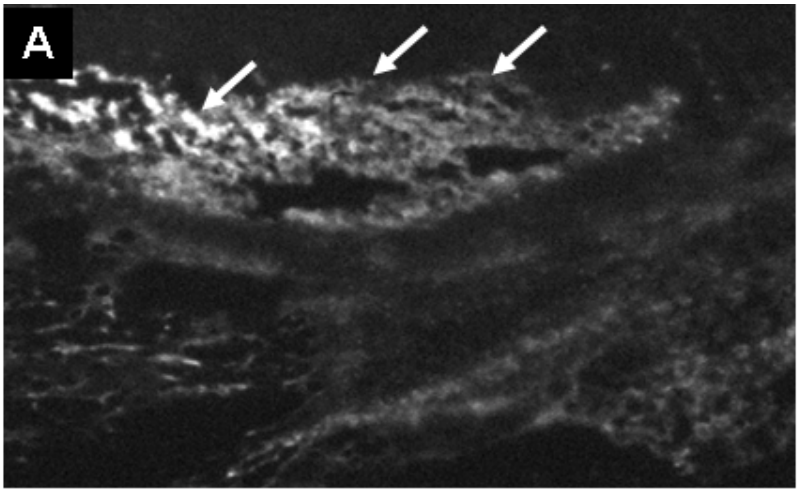

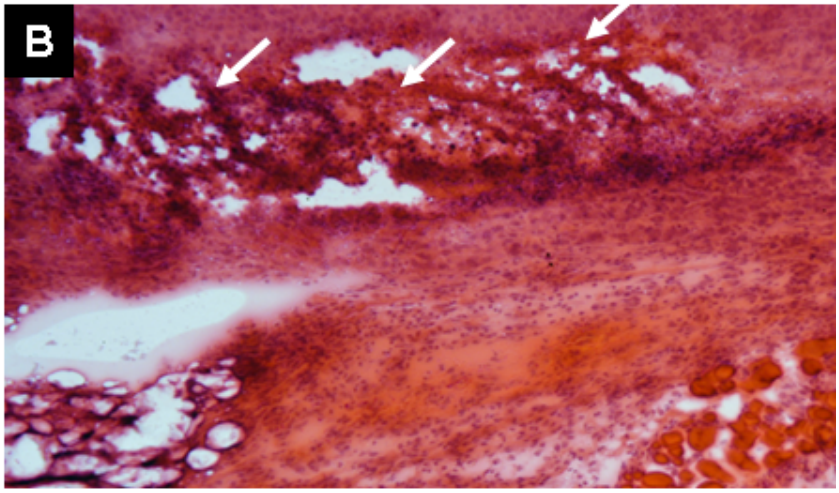

Supplemental Figure 6

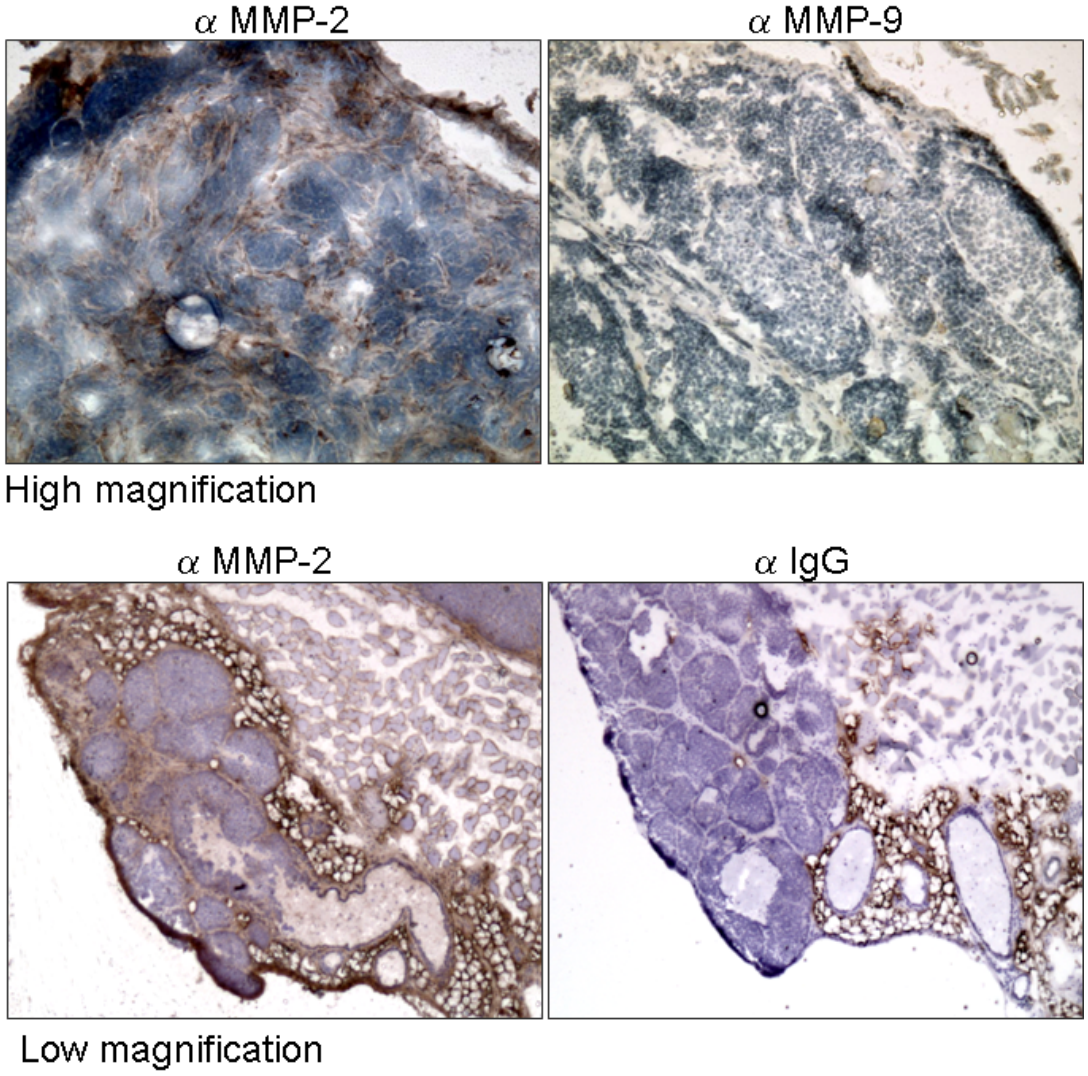

Supplemental Figure 7

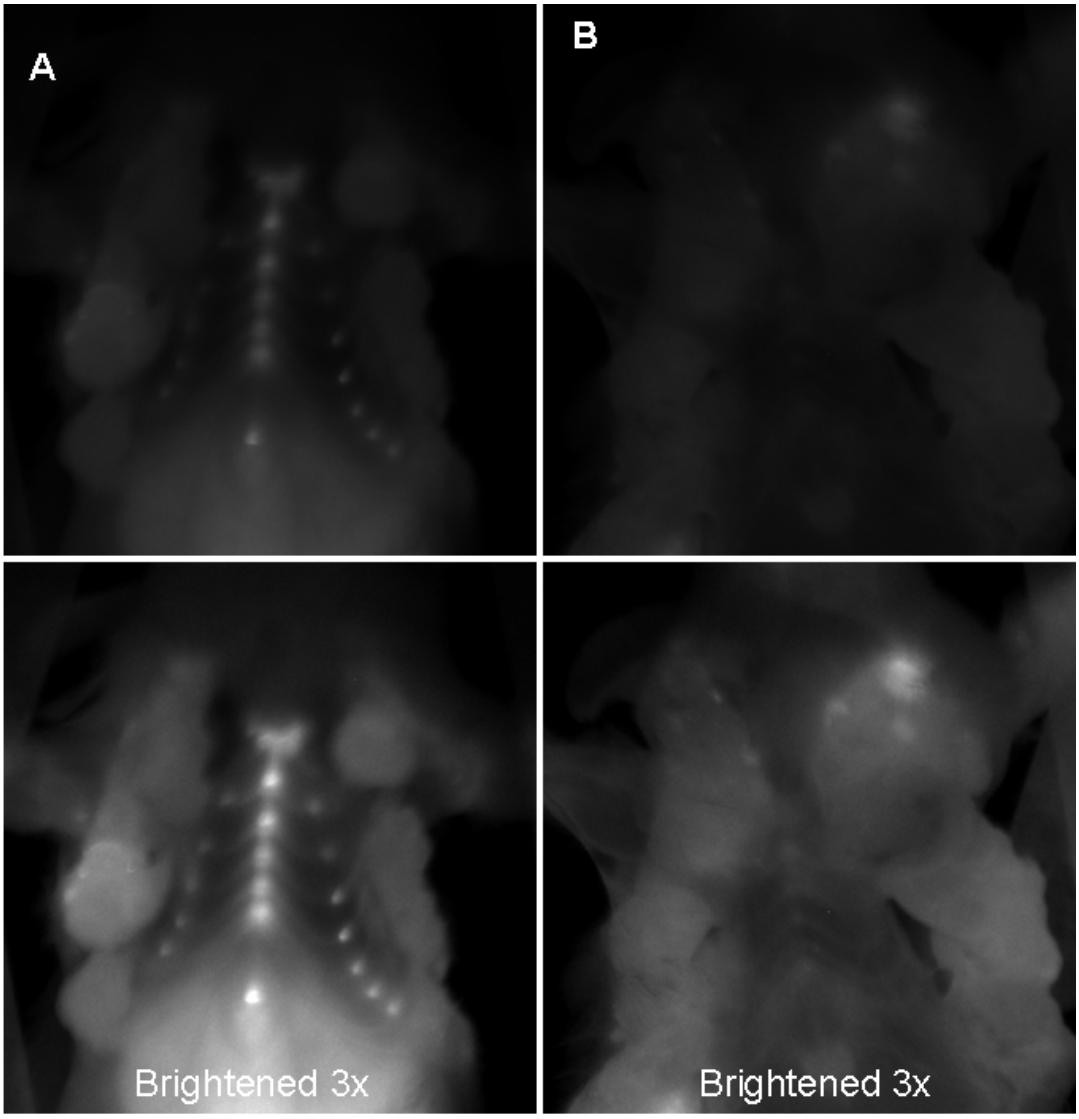

Supplemental Figure 8

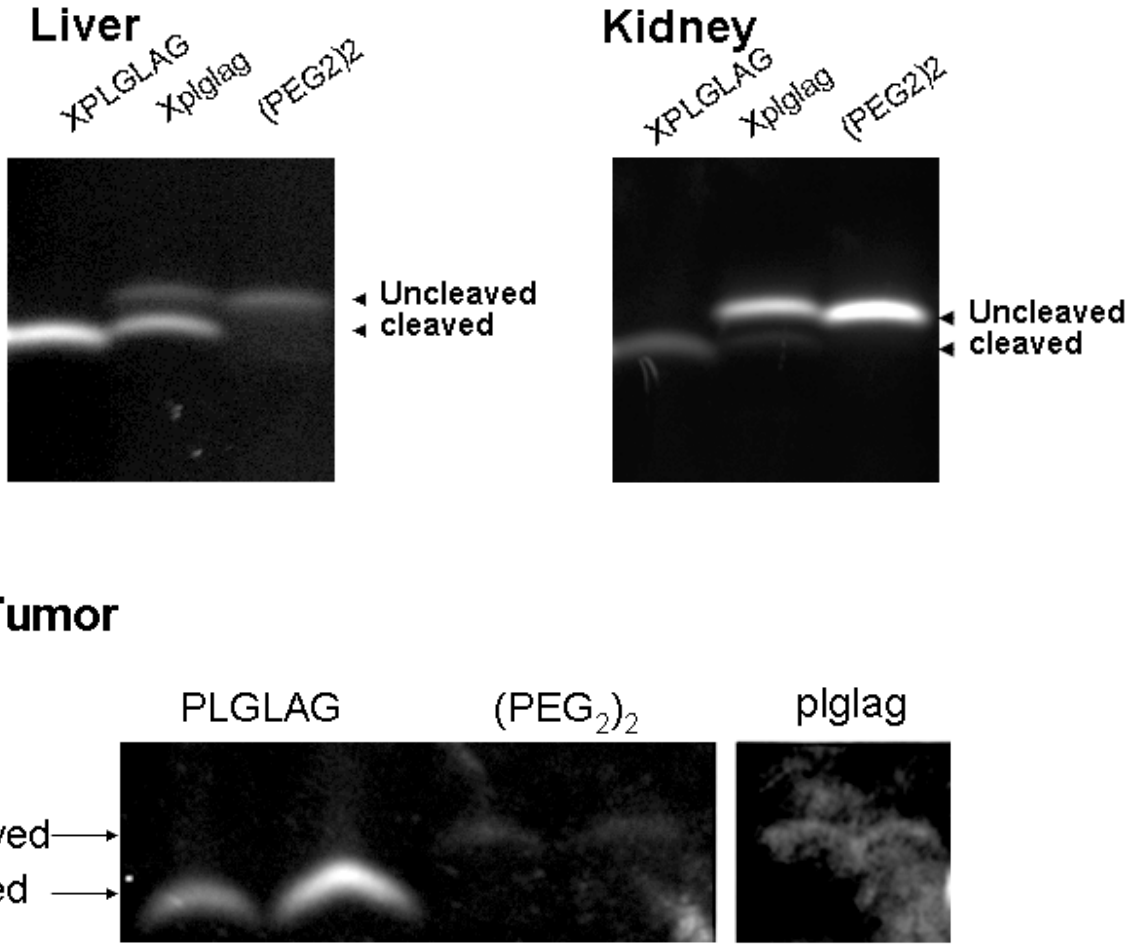

Supplemental Figure 9

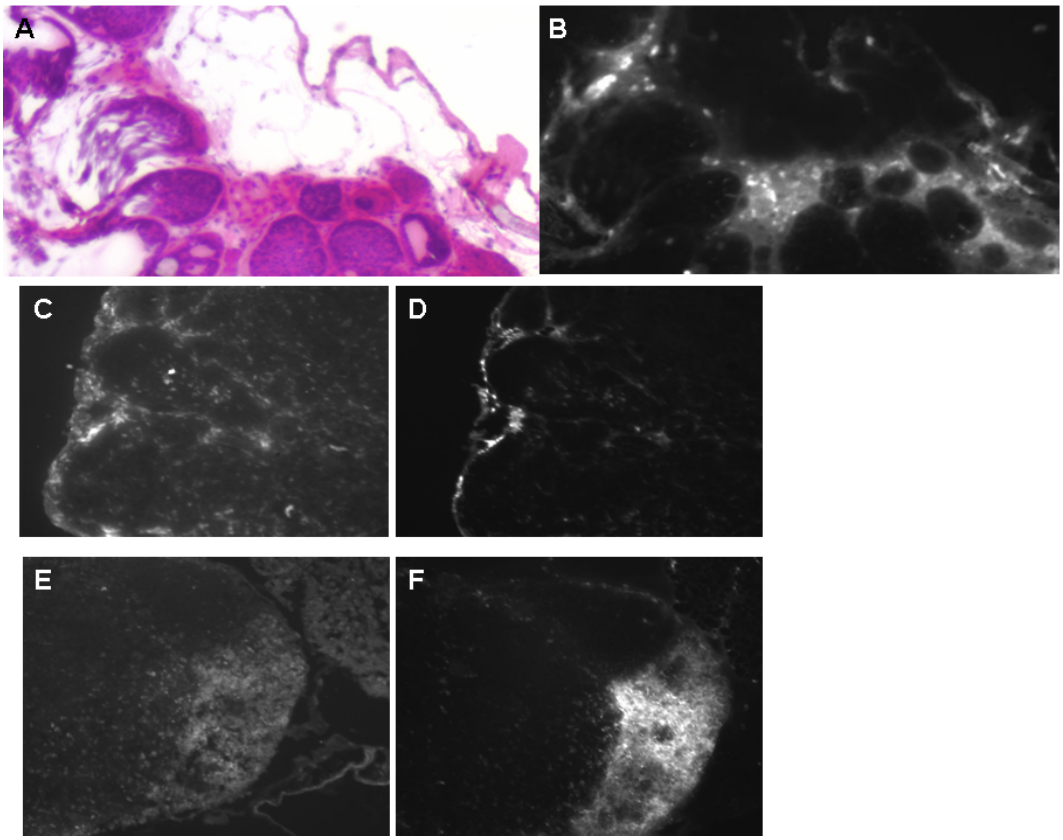

Supplemental Figure 10

Peptide LC Mass Spectra

Suc-e8-xplglag-r9-k(Cy5)
Found mass 3943

Chemical Formula: $C_{167}H_{273}N_{57}O_{50}S_2$
Exact Mass: 3941.00
Molecular Weight: 3943.44

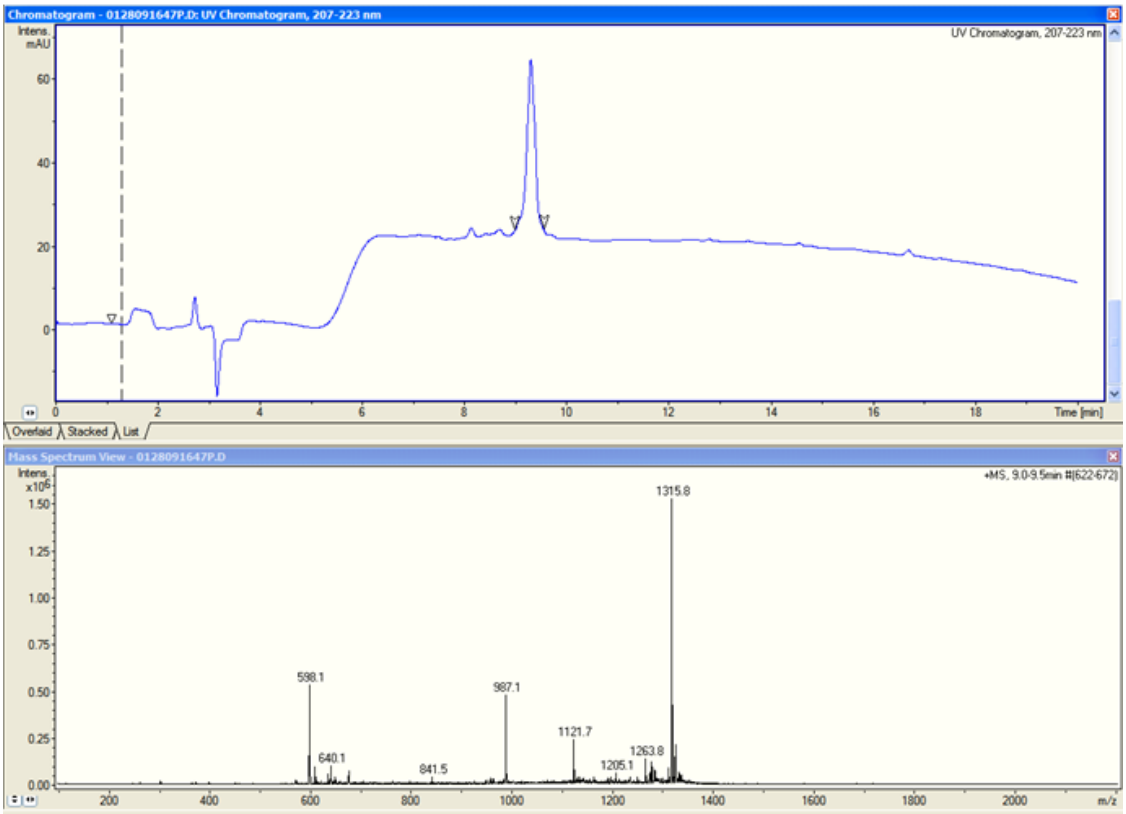

1842: Suc-e8-$(mPeg2)_2$-r9-k(Cy5)
Found mass 3728

Chemical Formula: $C_{152}H_{244}N_{52}O_{52}S_3$
Exact Mass: 3725.72
Molecular Weight: 3728.08

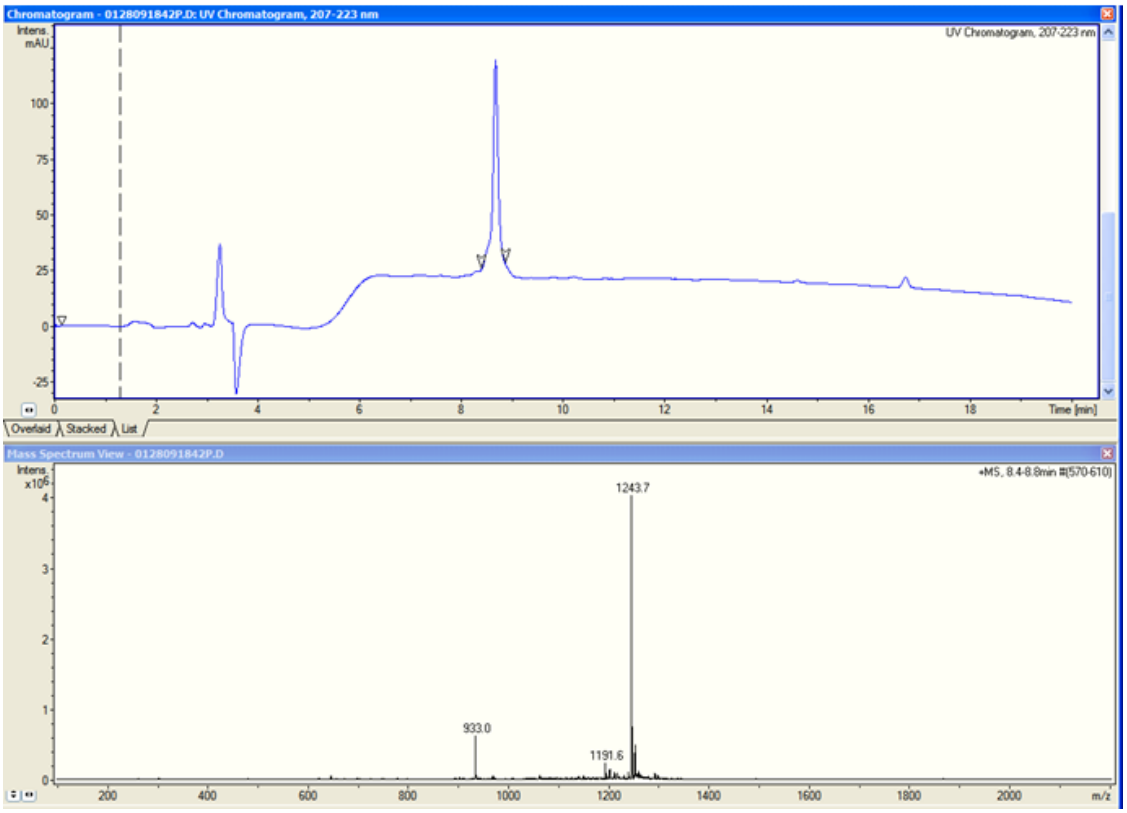

The m/z peaks at 1243.7 and 933.0 Da represent the molecule plus 3 or 4 protons ($M + 3H^+$ and $M + 4H^+$) respectively.

r9-c(Cy5)
Found mass 2304

Chemical Formula: $C_{96}H_{161}N_{42}O_{19}S_3$
Exact Mass: 2302.21
Molecular Weight: 2303.77

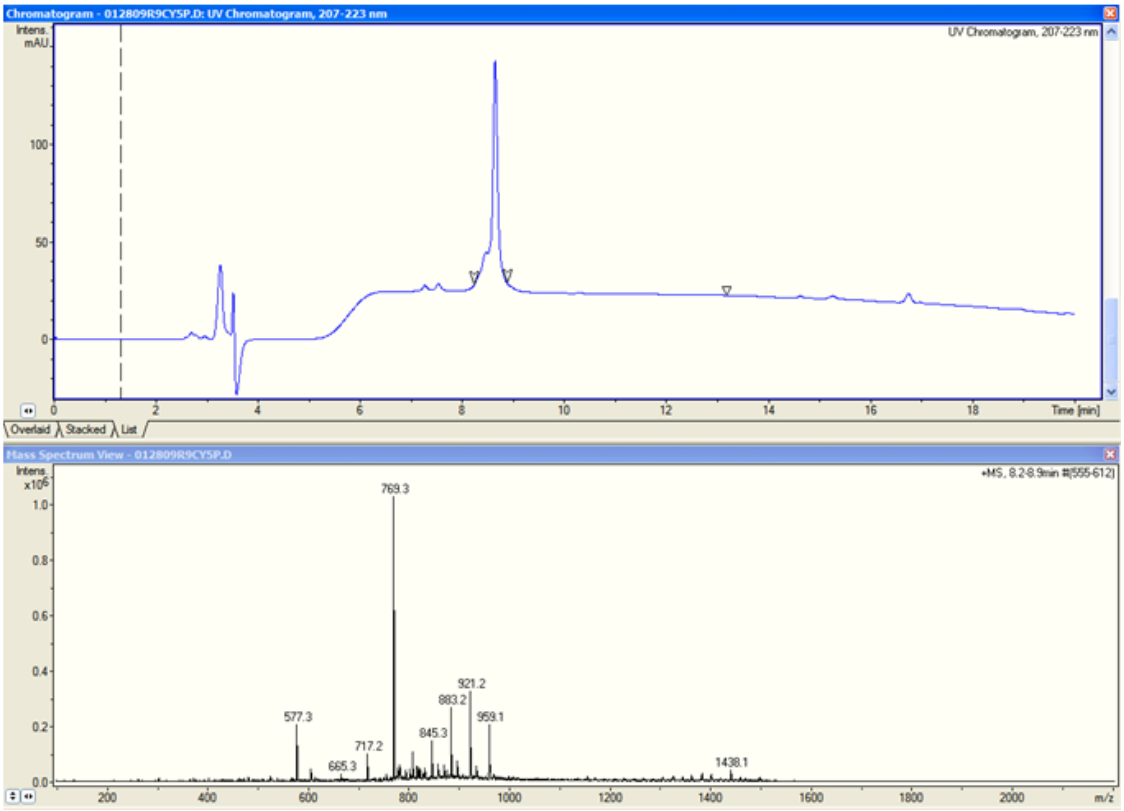

The m/z peaks at 769.3 and 577.3 Da represent the molecule plus 3 or 4 protons (M + $3H^+$ and M + $4H^+$) respectively.